J. Biochem. **139**, 857–864 (2006)
doi:10.1093/jb/mvj102

Conformational Change of the Loop L5 in Rice Kinesin Motor Domain Induced by Nucleotide Binding

Nobuhisa Umeki[1], Toshiaki Mitsui[1,*], Kazunori Kondo[2] and Shinsaku Maruta[2,*]
[1]Laboratories of Plant and Microbial Genome Control, Graduate School of Science and Technology, Niigata University, Niigata 950-2181; and [2]Division of Bioengineering, Graduate School of Engineering, Soka University, Hachioji, Tokyo 192-8577

Received January 10, 2006; accepted March 12, 2006

Loop L5 of kinesin is located near the ATPase site, in common with kinesins of various animal species. The rice plant-specific kinesin K16 also has a corresponding loop that is slightly shorter than that of mouse brain kinesin. The present study was designed to monitor conformational changes in loop L5 during ATP hydrolysis. For this purpose, we introduced one reactive cysteine into the L5 of rice kinesin and modified it with fluorescent probes. The cysteine in L5 was labeled with a fluorescent probe 2-(4′(iodoacetamide) anilino-naphthalene-6-sulufonic acid sodium salt) [IAANS]. IAANS was incorporated into L5 at an almost equimolar ratio in the absence of nucleotides. In contrast, the incorporated amount was reduced to 0.62 and 0.32 mol IAANS/mol motor domain in the presence of ATP and ADP, respectively. Upon nucleotide addition, the fluorescent intensity of IAANS incorporated into L5 was significantly reduced to 63% and 51% for ATP and ADP, respectively. These results suggest that L5 of rice kinesin significantly changes its conformation during ATP hydrolysis.

Key words: chemical modification, conformational change, fluorescent probe, kinesin, loop.

Abbreviations: DTT, dithiothreitol; EDTA, ethylendiaminetetraacetic acid; EGTA, ethylene glycol bis(β-aminoethyl ether)-*N,N,N′,N′*-tetraacetic acid; IAANS, 2-(4′(iodoacetamide)anilino-naphthalene-6-sulfonic acid sodium salt; IAANS-Q101C, Q101C labeled with IAANS; IAANS-WT, WT labeled with IAANS; K-16, rice-specific kinesin; MKH350, mouse brain kinesin motor domain; L5, loop 5; L12, loop12; Mant-8N_3-ADP, 3′-*O*-(*N*-methylanthraniloly)-2-azido-ADP; MT, microtubule; Ni-NTA, nickel nitrilotriacetic acid; Q101C, rice kinesin mutant (glutamine-to-cysteine substitution at residue 101); P_i, phosphate; SDS-PAGE, sodium dodecyl sulphate polyacrylamide gel electrophoresis; WT, wild type.

Kinesin is a motor protein that plays a significant role in intracellular transport, mitosis, meiosis, and axonal flow in the nervous system along microtubules, converting chemical energy from ATP into mechanical force. Kinesin is composed of two heavy chains and two light chains. The N-terminal 340 amino acid residues of the heavy chain form the globular domain, which contains the microtubule- and ATP-binding sites. The head domain of kinesin can be subdivided into the core of the catalytic domain of approximately 325 residues (which contains the microtubule- and ATP-binding sites), a linker region of 325–340 residues, and a connection to the neck region of 340–370 residues. Recent crystallographic studies have shown that kinesin (*1–4*) has striking structural similarity to the core of the catalytic domain of myosin and G-protein (*5*, *6*). This similarity suggests that these motor proteins and molecular switches, which convert energy from ATP into force production for motility and switching, use a similar conformational strategy at the first stage of energy transduction. On the other hand, kinesin has several unique loops, L5 and L12 (*4*). L5 is located near the ATP-binding site, and L12 in the microtubule-binding site (Fig. 1) (*4*). Similarly, myosin has several unique loops: loop B (aa 320–327), M (aa 677–689), and N (aa 127–136), in the region of the ATP-binding cleft, which are not present in kinesin (*4*). The precise function of these loops remains unclear; however, they may determine the characteristic properties of motor proteins, such as mediating the interaction between ATP- and microtubule-binding sites or ATP- and actin-binding sites.

We demonstrated previously that a fluorescent-labeled photoreactive ADP analogue, Mant-8-N_3-ADP, specifically crosslinks to loop M of skeletal muscle (*7*). The fluorescent ADP derivative was used as a probe to monitor actin-induced conformational changes in loop M (*7*). Analysis of actin-induced changes in Mant-group fluorescence polarization, acrylamide-induced quenching, and fluorescence energy transfer confirmed that actin binding induces conformational changes in loop M that result in the displacement of Mant-8-N_3-ADP from the ATP-binding cleft (*8*).

We observed that point mutations in mouse brain kinesin at Pro 103 and Leu 105 in L5 (96–106) significantly affect ATPase activity (unpublished data). On the other hand, the kinesins point mutated at Leu 100 and His 101 retained normal ATPase properties. Moreover, the fluorescence spectrum of Trp-substituted Leu 100 in L5 was significantly altered in a nucleotide-dependent manner reflecting the physiological conformational change during ATP hydrolysis (unpublished data). Therefore, it is

*To whom correspondence should be addressed. Fax: +81-426-91-9312, E-mail: shinsaku@t.soka.ac.jp (Shinsaku Maruta); Fax: +81-25-262-6641, E-mail: t.mitsui@agrews.agr.niigata-u.ac.jp (Toshiaki Mitsui).

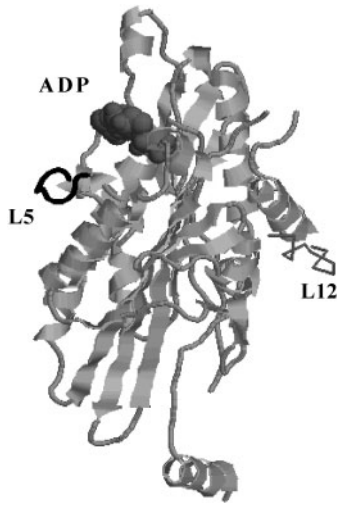

Fig. 1. **Location of L5 in the crystal structure of kinesin motor domain.** The L5 is shown in black in the cartoon model of the kinesin motor domain. The ADP and L12 (one of the microtubule-binding sites) are represented in the space-filling model and stick model, respectively. The structure was prepared using the molecular graphic program Ras Mac v2.6 using the coordinate data (rattus norvegicus kinesin: 2KIN) in the protein data bank database.

thought that the anterior half of the loop does not influence the ATPase cycle, but the posterior half of the loop, which is closer to the ATPase site, does influence the ATPase cycle. Comparative studies on primary kinesin structures derived from several different species revealed that the bulge loop L5 of the plus-end directed kinesins is generally longer than that of minus-end directed kinesins (*9*). We recently expressed the motor domain of rice specific kinesin K-16 and characterized its properties (*10*). Rice kinesin also has a conserved L5 that is slightly shorter than that found in mouse brain kinesin.

The aim of the present study was to investigate the conformational change of L5 that may be related to kinesin-specific motile function. For this purpose, we introduced a reactive cysteine residue into L5, and used cysteine labeled with the environmentally sensitive fluorescent probe, IAANS, which has been widely used for protein structural studies (*11–13*). Studies of fluorescent spectra, fluorescent polarization, and fluorescent quenching of the probe in L5 clearly demonstrated that L5 changes its conformation during ATP hydrolysis.

MATERIALS AND METHODS

Expression and Purification of Rice Kinesin Mutant Q101C—The Q101C rice kinesin mutant plasmid was constructed by introducing a single amino acid change in the wild-type (WT) rice kinesin K16 plasmid (Accession No. AK068672), which was supplied by the National Institute of Agrobiological Science (Tsukuba, Japan). The glutamine-to-cysteine substitution at residue 101 was verified by DNA sequencing. DNA sequencing was confirmed by the dideoxy chain termination method with a SQ-5500 sequencer (Hitachi, Tokyo) using the Genetyx program (Software Development). The Q101C plasmid and WT rice kinesin plasmid were transformed into *Escherichia coli* BL21 (DE3) pLysE for expression. The Q101C and WT rice kinesin were purified by Ni-NTA metal affinity chromatography according to the method of Shibuya *et al.* (*14*). Purity was assessed by sodium dodecyl sulfate polyacrylamide gel electrophoresis (SDS-PAGE), which revealed a single band on Coomassie-stained gels. Samples were dialyzed against 120 mM NaCl, 30 mM Tris-HCl, pH 7.5, and 1 mM dithiothreitol (DTT), and stored at −80°C until use. Tubulin was purified from porcine brain as described by Hackney (*15*).

Chemicals—Restriction enzymes and other enzymes were purchased from Toyobo (Tokyo) unless otherwise stated. Oligonucleotides were synthesized by Sawady (Tokyo). The nickel-chelating column was purchased from Sigma (St. Louis, MO). *E. coli* BL21 (DE3) pLysE and pET21a vector were purchased from Novagen (Madison, WI). All chemicals were purchased from Wako Pure Chemicals (Osaka, Japan) unless otherwise stated. ATP and ADP were purchased from Oriental Yeast (Osaka). 2-(4′(iodoacetamide) anilino-naphthalene-6-sulfonic acid sodium salt) (IAANS) was purchased from Molecular Probes (Eugene, OR). BCA protein concentration assay was from Pierce (Rockford, IL).

Measurement of Fluorescence—Fluorescence was measured with an RF-5000 spectrofluorophotometer (Shimadzu, Tokyo) and F-2500 spectrofluoro-photometer (Hitachi, Tokyo). Unless otherwise stated, all fluorescence measurements were carried out in a buffer containing 120 mM NaCl, 30 mM Tris-HCl, pH 7.5, and 2 mM $MgCl_2$ at 25°C. Excitation and emission wavelengths were 330 nm and 450 nm, respectively.

Fluorescence polarization: Fluorescence polarization was measured with an RF-5000 spectrofluorophotometer (Shimadzu, Tokyo) and F-2500 spectrofluorophotometer (Hitachi, Tokyo) attached polarizer. Steady-state polarized light was used to excite IAANS-rice-kinesin; the intensity of emitted fluorescence was measured at both horizontal (I_h) and vertical (I_v) angles to the incident polarized plane. The excitation wavelength was 330 nm (band width, 10 nm); fluorescent emission was detected at 450 nm (band width, 20 nm). Fluorescence polarization (P) was calculated from the following equation: $P = (I_h - I_v)/(I_h + I_v)$

Acrylamide quenching: Acrylamide (0–100 mM) quenching of IAANS fluorescence was analyzed according to Stern and Volmer (*16*, *17*). The Stern-Volmer quenching constant (K_{SV}) was calculated from the following equation: $F_0/F = 1 + K_{SV}[Q]$, where F_0 and F are fluorescence intensities in the absence and presence of the quencher, respectively, and [Q] is the concentration of acrylamide.

Fluorescence Labeling of Q101C Kinesin and WT Rice Kinesin with IAANS—Q101C kinesin and WT kinesin motor domains (10 μM) were incubated with 80 μM IAANS for 30 min at 25°C in a buffer comprising 120 mM NaCl, 30 mM Tris-HCl, pH 7.5, and 2 mM $MgCl_2$. The reaction was stopped by addition of 2 mM DTT. Unbound IAANS was removed by centrifugal gel filtration on a Sephadex G-50 spin column equilibrated with 120 mM NaCl and 30 mM Tris-HCl, pH 7.5. The amount of incorporated IAANS was estimated using the absorption coefficient at 326 nm of 27,000 $M^{-1}\cdot cm^{-1}$ for the IAANS group (*18*).

ATPase Assay—Rice kinesin (1 μM) and MKH350 (1 μM) were preincubated for 5 min in 10 mM imidazole-HCl,

pH 7.0, 50 mM KCl, 3 mM $MgCl_2$, 0.1 mM ethylenediaminetetraacetic acid (EDTA), 1 mM ethylene glycol bis (beta-aminoethyl ether)-*N*,*N*,*N*′,*N*′-tetraacetic acid (EGTA), 1 mM β-mercaptoethanol, and 5 μM microtubules. The ATPase reaction was initiated by the addition of 2 mM ATP at 25°C. The reaction was stopped by the addition of 10% trichloroacetic acid, and the released Pi measured by the method of Youngburg and Youngburg (*19*).

RESULTS

Preparation of a Rice Kinesin Mutant with Cysteine in L5—The wild-type rice kinesin K-16 motor domain has two intrinsic cysteines at positions 214 and 301. We confirmed first that the cysteine residues were scarcely reactive with SH-reactive reagents. Therefore, we constructed a cDNA encoding motor domain rice kinesin, in which Gln101 corresponding to Leu100 of mouse brain kinesin was replaced by Cys, without removing the intrinsic cysteines. The constructed cDNA was transformed into *E. coli* BL21 (DE3) pLysE. The expressed Q101C rice kinesin was purified by Ni-NTA metal affinity chromatography, and kinesin mutant ATPase activity was measured in the presence of various concentrations of microtubules to determine whether the mutant retained normal enzymatic properties. As shown in Fig. 2, the basal steady-state ATPase activity in the absence of microtubules and the pattern of microtubule-stimulation of the ATPase activity of Q101C were similar to those of the WT rice kinesin K16 motor domain. The mutant Q101C retained native enzymatic properties. The maximal ATPase activity and the microtubule concentration for half maximal stimulation of the kinesins were estimated from Fig. 2. V_{max} and K_{MT} of Q101C were 0.99 s^{-1} and 4 μM, respectively, which were almost identical to those of WT. These results indicate that the mutant retains native enzymatic properties.

Labeling of the Cysteine Residue in L5 by Fluorescent Probe—In order to determine the optimal conditions for specific labeling of the cysteine residue in L5, we conducted time-course studies of the reaction- and concentration-dependency of IAANS. Figure 3A shows the time-course labeling of Q101C and WT kinesin motor domain with IAANS, performed at 25°C with an 8-fold excess of IAANS over kinesin. The amount of incorporated IAANS was estimated using the absorption coefficient at 326 nm of 27,000 $M^{-1}\cdot cm^{-1}$ for the IAANS group (*18*). The cysteine residue additionally incorporated into L5 by molecular biological technique was highly reactive and labeled almost stoichiometrically by SH group specific reactive fluorescent probe IAANS. As shown in Fig. 3A (solid circles), the time-course incorporation of IAANS was biphasic. The first phase rapidly reached a stoichiometric amount, and the second phase increased slowly corresponding to WT incorporation. Subtracting the values of open circles from the closed circles at each reaction time showed a saturated incorporation of IAANS at the stoichiometrical molar ratio. However, the ATPase activity of Q101C was not significantly affected by modification of IAANS. Furthermore, basal and MT-activated ATPase were slightly reduced, at less than 10–20%, even at long reaction time when 101C in L5 was almost fully modified by IAANS, suggesting retention of the native enzymatic properties.

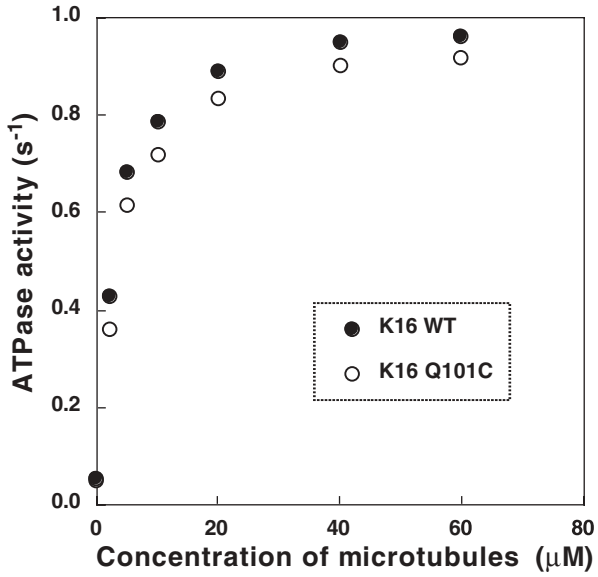

Fig. 2. **Microtubule concentration dependence of the ATPase activity of the rice kinesin Q101C mutant.** The ATPase assay was carried out at 25°C in 30 mM Tris-HCl, pH 7.5, 3 mM $MgCl_2$, 0.1 mM EDTA, 1 mM EGTA, 1 mM β-mercaptoethanol, 1 μM K16MD and 0–60 μM microtubule. The ATPase reactions were started by adding 2 mM ATP. For K16WT (closed circles), the estimated maximum rate and [K_m (MT)] were 0.99 s^{-1} and 4 μM, respectively. For K16 Q101C (open circles), the maximum rate and [K_m (MT)] were 0.97 s^{-1} and 4 μM, respectively.

As shown in Fig. 3B, incorporation of IAANS into the cysteine residue in L5 was saturated at lower concentrations of IAANS than the corrected value obtained by subtracting the data of WT from the corresponding value of Q101C. These results suggest that at lower concentration of IAANS and for short reaction times, incorporation of IAANS into the two intrinsic cysteines is negligible, and only the cysteine residue in L5 of Q101C is specifically labeled by IAANS.

Interestingly, the presence of nucleotides significantly affected the binding of IAANS into the cysteine in L5. As shown in Fig. 3C, the amount of incorporated IAANS in the presence of ATP and ADP was reduced to 70% and 50%, respectively. Binding of IAANS into the intrinsic cysteine of WT was not affected by the addition of nucleotides. These results indicate that the region of the cysteine residue in L5 changes its conformation during ATP hydrolysis.

Nucleotide-Induced Fluorescence Changes in IAANS-Q101C—Next, we examined the effect of nucleotides on the emission spectra of IAANS-Q101C. As shown in Fig. 4A, ATP reduced the fluorescence intensity of IAANS-Q101C by 38%. This decrease was accompanied by a blue shift of the emission maximum from 449 to 446 nm. Interestingly, the fluorescence intensity further decreased in the presence of ADP by 47% and produced a blue shift of the emission maximum to 444 nm. The spectral change upon the addition of ADP indicated that the ATPase site of the IAANS-Q101C was vacant. To confirm this, the IAANS-Q101C was treated with EDTA to remove entrapped ADP from the ATPase site. As shown in Fig. 4A (line 4), upon the addition of ADP, fluorescence intensity of

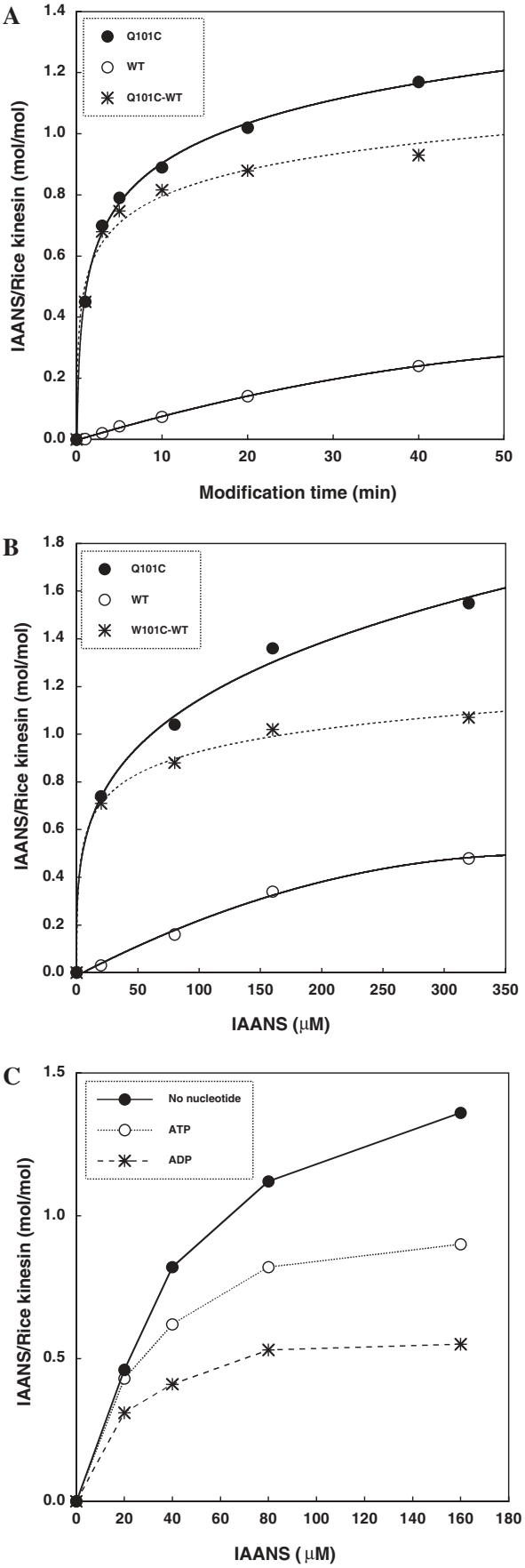

EDTA-treated IAANS-Q101C decreased relatively to the same level as that of before treatment with EDTA, indicating that the kinesin does not contain ADP. Further confirmatory experiments to show that kinesin does not contain ADP were performed using ultrafiltration. ADP was incubated with equimolar Q101C and the solution was passed through an ultrafiltration filter to remove the high molecular weight kinesin. As shown in Fig. 5 (broken line), no absorption was observed at 260 nm of ADP in the filtrate resulting from ADP binding to Q101. In contrast, ADP did not bind to heat-denatured Q101C (Fig. 5, dotted line). These results clearly demonstrated that the rice kinesin motor domain prepared in the absence of MgATP as described in "MATERIALS AND METHODS" has a vacant ATPase site and does not contain ADP. We have also prepared the MgADP-bound rice kinesin motor domain in the presence of Mg and ATP, and compared it with MgADP-free kinesin. Interestingly, the nucleotide-free kinesin showed almost the same stability as the nucleotide-bound kinesin. The kinesin purified in the presence of MgATP showed almost the same MT-dependent ATPase activities as shown in Fig. 6A. Moreover, the stability of MgADP-free kinesin upon long-term incubation at 25°C was almost the same as that of Mg-ADP bound kinesin. As shown in Fig. 6B, the microtubule-dependent ATPase activity was almost 100% even after 12 h of incubation. Therefore, it was clearly demonstrated that the nucleotide free rice kinesin motor domain is as stable as the Mg-ADP bound rice kinesin.

Fluorescence of IAANS bound to WT was negligible (Fig. 4A, lines 5 and 6). IAANS is an environmentally sensitive fluorescent probe that is covalently linked to the cysteine residue in L5, and the fluorescent changes reflect changes in hydrophobicity around the probe due to changes in conformation. Hence, changes in fluorescence derived from IAANS bound to 101C in L5 resulted in conformational change of L5 induced by nucleotide binding. We also observed similar results for L5 of mouse brain kinesin MKH350. Prior to fluorescent measurement, the MKH350 mutant H101C was treated with EDTA to remove ADP entrapped in the ATPase site. As shown Fig. 4B, upon

Fig. 3. **A: Time course of incorporation of IAANS into the L5 of the rice kinesin.** Rice kinesin Q101C or rice kinesin WT (each 10 μM) was modified with an 8-fold molar excess of IAANS at 25°C in a buffer of 120 mM NaCl and 30 mM Tris-HCl, pH 7.5. The reaction was stopped by the addition of 2 mM DTT. Unbound IAANS was removed by centrifugal gel filtration on Sephadex G-50 column equilibrated with 120 mM NaCl and 30 mM Tris-HCl, pH 7.5. The amount of incorporated IAANS was estimated by using the absorption coefficient at 326 nm of 27,000 $M^{-1}\cdot cm^{-1}$ for the IAANS group. Q101C, solid circles; rice kinesin WT, open circles; Q101C-WT, asterisk. **B: Concentration-dependent incorporation of IAANS into the L5 of the rice kinesin.** 10 μM rice kinesin was reacted with 20, 80, 160 and 320 μM IAANS at 25°C in a buffer of 120 mM NaCl and 30 mM Tris-HCl, pH 7.5, for 30 min. Subsequent procedures were performed as described in the legend of (A). **C: Nucleotide-dependent incorporation of IAANS into the L5 of the rice kinesin.** Rice kinesin (10 μM) was reacted with 20, 40, 80 and 160 μM IAANS at 25°C in a buffer of 120 mM NaCl, 30 mM Tris-HCl, pH 7.5, and 3 mM $MgCl_2$, in presence or absence 2 mM nucleotide for 30 min. Subsequent procedures were performed as described in the legend of (A).

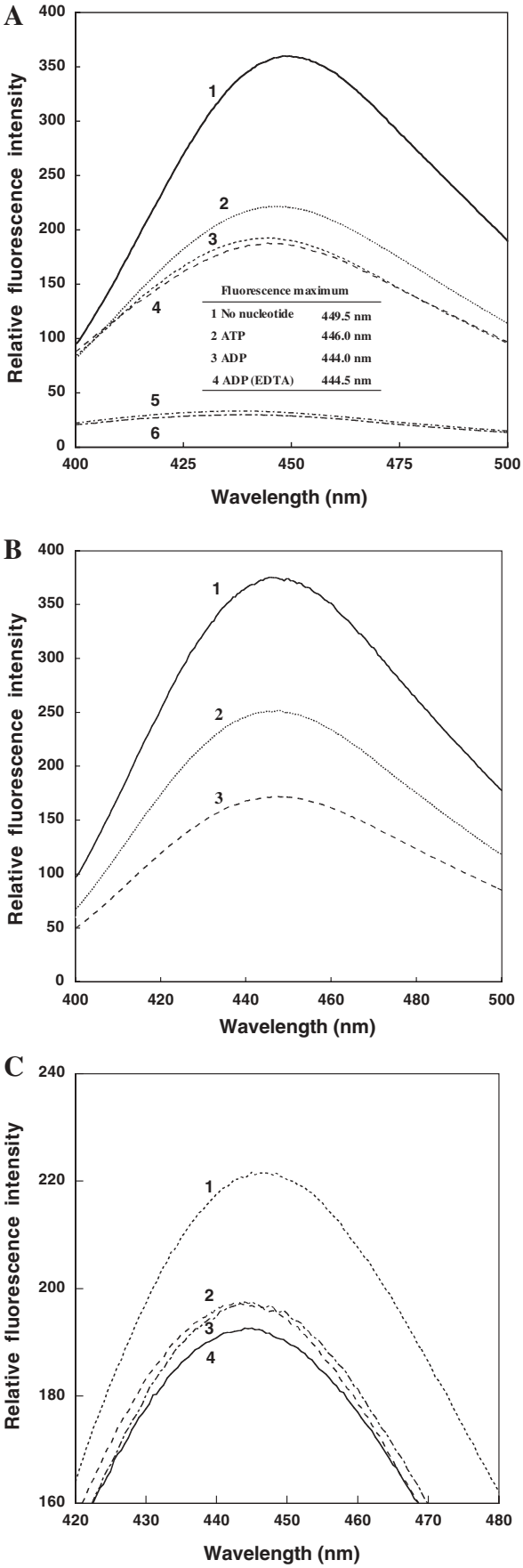

addition of nucleotides, the fluorescence of IAANS-labeled H101C showed similar reduction to that of rice kinesin Q101C. We also examined the effect of the ATP analogues, ATPγS and AMP-PNP. It is known that ATPγS is hydrolyzed slowly by ATPase, while AMP-PNP is a non-hydrolyzable ATP derivative. Fluorescence intensities of IAANS-kinesin in the presence of ATPγS and AMP-PNP were slightly higher than that in the presence of ADP as shown in Fig. 4C. However, no significant difference in the spectra between ATPγS and AMP-PNP was observed.

Acrylamide Quenching of IAANS-Q101C Fluorescence—As described above, the IAANS fluorophore bound to 101C sensed different environments in L5 induced by nucleotides. To obtain further details about the different environments, we examined the accessibility of the IAANS fluorophore in L5 from the extent of fluorescence quenching by solute quencher. Fluorescence of IAANS-Q101C was measured in the presence of various concentrations of acrylamide as a quencher. Data were analyzed by calculation of Stern-Volmer quenching constants (K_{sv}) from the plots of relative fluorescence versus acrylamide concentration (Fig. 7). The value of K_{sv} for IAANS-Q101C in the absence of nucleotide was 2.6 M^{-1}. In contrast, in the presence of 1 mM ATP and 1 mM ADP, the values of K_{sv} for IAANS-Q101C increased to 3.6 M^{-1} and 3.5 M^{-1}, respectively. These results suggest that the fluorophore is more accessible in the presence of nucleotides than in their absence. However, there were no significant differences in accessibility between ATP and ADP.

Fluorescence Polarization of IAANS-Q101C—Fluorescence polarization was used to measure the effects of nucleotides on the mobility of IAANS attached to 101C in L5. Fluorescence polarization was significantly increased when IAANS attached to 101C (Fig. 8, bar 3),

Fig. 4. **A: Fluorescence emission spectra of rice kinesin labeled at loop 5 with IAANS.** IAANS-Q101C and IAANS-WT were prepared as described in "MATERIALS AND METHODS." Fluorescence emission spectra of rice kinesin labeled at loop 5 with IAANS were monitored in a solution of 120 mM NaCl, 30 mM Tris-HCl pH 7.5, 2 mM $MgCl_2$, 1 μM rice kinesin-IAANS at 25°C. IAANS was excited at 330 nm, and the emission spectra were measured at 400–500 nm. (1) 1 μM rice kinesin IAANS-Q101C. (2) 1 μM rice kinesin IAANS-Q101C + 1 mM ATP. (3) 1 μM rice kinesin IAANS-Q101C + 1 mM ADP. (4) 1 μM rice kinesin IAANS-Q101C (EDTA treated) + 1 mM ADP. (5) 1 μM rice kinesin IAANS-WT. (6) 1 μM rice kinesin IAANS-WT + 1 mM ATP. Fluorescence emission maxima of IAANS-Q101C in the presence of nucleotides were as follows: 449.5 nm (no nucleotide), 446.0 nm (presence 1 mM ATP), 444.0 nm (presence 1 mM ADP). **B: Fluorescence emission spectra of mouse kinesin MKH350 mutant H101C labeled at loop 5 with IAANS.** The mouse kinesin MKH350 labeled at loop 5 with IAANS was treated with EDTA to remove entrapped ADP completely prior to fluorescence measurement. Fluorescence emission was measured as described in the legend of (A). (1) 1 μM IAANS-H101C. (2) 1 μM IAANS-H101C + 1 mM ATP. (3) 1 μM IAANS-H101C + 1 mM ADP. **C: Effect of AMP-PNP and ATPγS on the fluorescence spectra of rice kinesin labeled at L5 with IAANS.** Fluorescence emission spectra were measured under the same conditions as described in (A). (1) 1 μM Q101C-IAANS + 1mM ATP. (2) 1 μM Q101C-IAANS + 1 mM ATPγS. (3) 1 μM Q101C-IAANS + 0.5 mM AMP-PNP. (4) 1 μM Q101C-IAANS + 1 mM ADP. Fluorescence emission maxima of IAANS-Q101C in the presence of nucleotides were as follows: 446.0 nm (ATP), 443.5 nm (ATPγS), 443.5 nm (AMP-PNP), 444.0 nm (ADP).

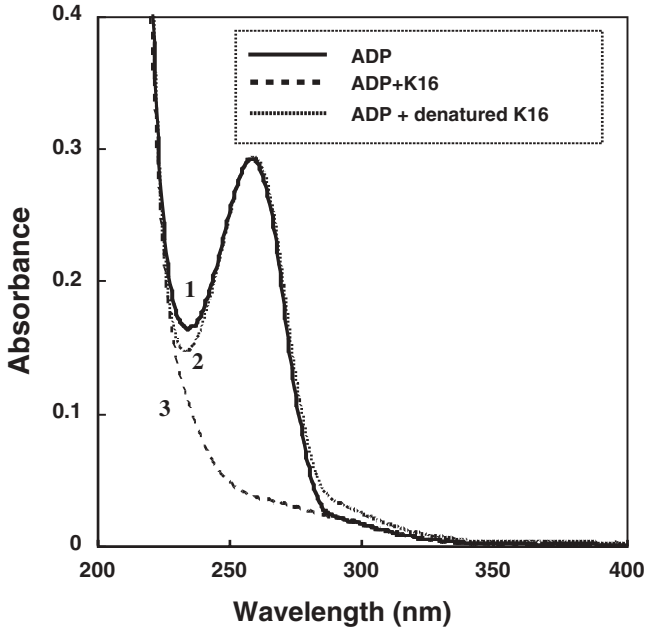

Fig. 5. **Binding of ADP to the vacant ATPase site of rice kinesin motor domain.** To show that the rice kinesin K16 does not contain ADP, ADP binding was monitored using ultrafiltration. ADP and K16 motor domain (20 μM) were incubated in a solution of 120 mM NaCl, 30 mM Tris-HCl, pH 7.5, 2 mM $MgCl_2$, and 0.2 mM DTT, and then subjected to ultra-filtration (Ultrafree-MC, Millipore, Bedford, MA), which allows passage of small molecules of less than 10,000 in molecular weight. The absorption spectra of the ultrafiltration permeates were measured. (1) 20 μM ADP, (2) 20 μM ADP + heat denatured 20 μM K16, (3) 20 μM ADP + 20 μM K16.

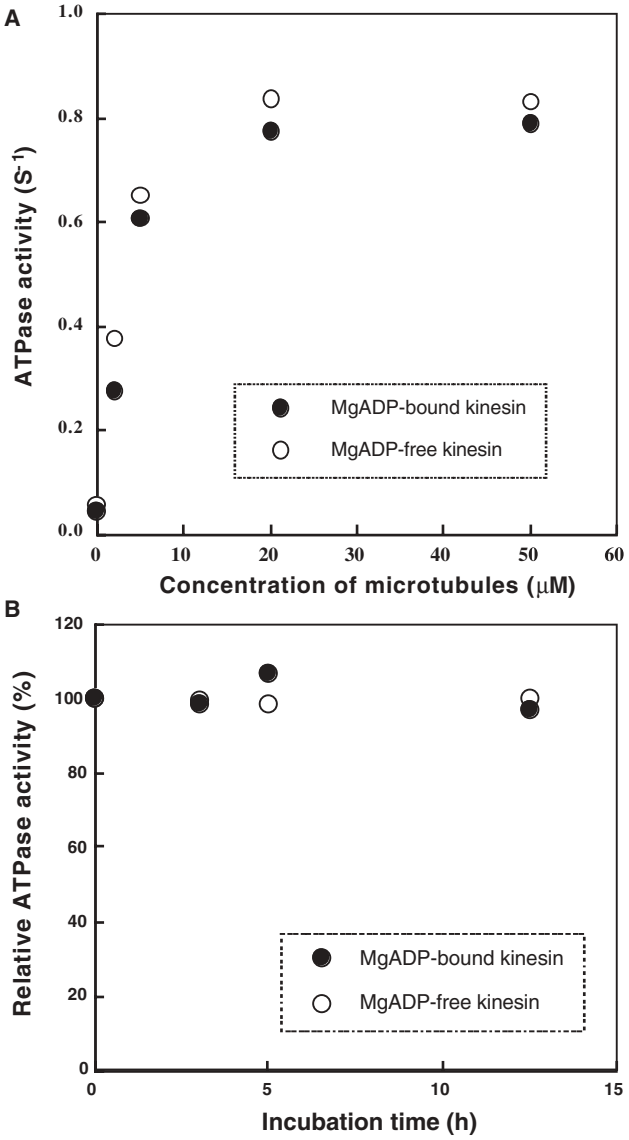

Fig. 6. **A: Microtubule dependent ATPase activity of the ADP-free rice kinesin and ADP-bound rice kinesin.** ADP-free K16MD and ADP-bound K16MD were prepared in the presence or absence of 0.1 mM MgATP. The ATPase assay was carried out at 25°C in 30 mM Tris-HCl pH 7.5, 3 mM $MgCl_2$, 0.1 mM EDTA, 1 mM EGTA, 1 mM β-mercaptoethanol, 1 μM K16MD and 0–50 μM microtubules. The ATPase reaction was started by adding 2 mM ATP. For the ADP-free K16MD (closed circles), the maximum rates and [K_m (MT)] were about 0.8 s^{-1} and about 4 μM, respectively. For the ADP-bound K16MD (open circles), the maximum rate constants and [K_m (MT)] were about 0.81 s^{-1} and 4 μM , respectively. **B: Stability of the ADP-free rice kinesin.** ADP-free K16MD (open circles) and ADP-bound K16MD (closed circles) were incubated in 120 mM NaCl, 30 mM Tris-HCl pH7.5, 0.1 mM $MgCl_2$, (0.1 mM ATP) for 0, 3, 5 and 12.5 h at 25°C. The ATPase assay was carried out at 25°C in 30 mM Tris-HCl pH 7.5, 3 mM $MgCl_2$, 0.1 mM EDTA, 1 mM EGTA, 1 mM β-mercaptoethanol, 1 μM K16MD and 10 μM microtubules. The ATPase reaction was started by addition of 2 mM ATP.

compared with free IAANS (Fig. 8, bar 1). This increase in polarization reflected the large reduction in rotational mobility of the probe resulting from its incorporation into a macromolecule of protein. The addition of 1 mM ADP slightly increased fluorescence polarization (Fig. 8, bar 5), and the addition of 1 mM ATP resulted in a slight and further increase in fluorescence polarization. These results suggest that the nucleotides induced a conformational change at L5 that results in decreased probe mobility. As a control, we measured the fluorescence polarization of guanidine-HCl–denatured IAANS-Q101C (Fig. 8, bar 2). These results showed very low polarization, confirming that the polarization measurements reflect the mobility of the IAANS-group in L5.

DISCUSSION

The aim of the present study was to investigate the conformational change of L5 that may be related to the kinesin-specific motile function. Recent studies suggested the potential roles of the loops from functional proteins. Cooperative swinging of the paired loops of the mitochondrial ATP/ADP carrier appears to mediate the protein's transport function (*20*). A similar loop structure may be involved in ion channel function in colicin Ia (*21*). These findings suggest that L5 of kinesin, uniquely located in the vicinity of the ATP-binding site (Fig. 1), may also determine the characteristic properties of motor activity. Point mutations in the region of the posterior half of the L5 change the ATPase activity and microtubule interactions (our unpublished data). Therefore, the L5 may have an important function in kinesin. However, the molecular

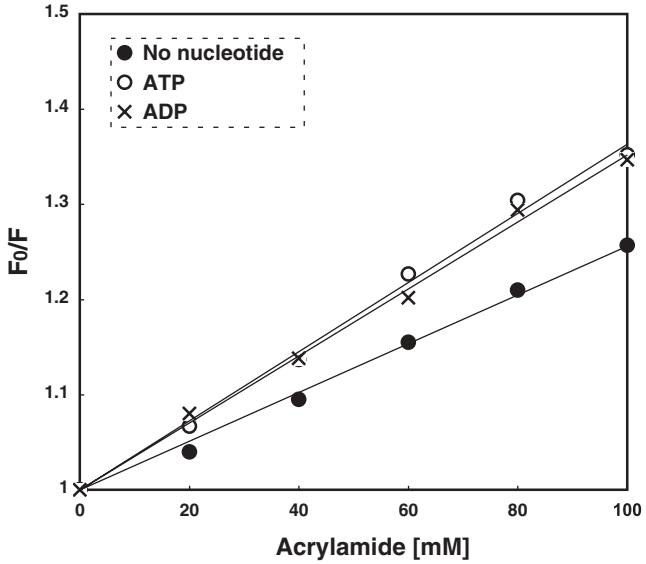

Fig. 7. **Stern-Volmer plots of acrylamide quenching of the fluorescence of IAANS attached to 101C in L5.** The assay was performed in a buffer of 120 mM NaCl, 30 mM Tris-HCl, pH 7.5, and 2 mM $MgCl_2$, with or without of 2 mM nucleotide. IAANS-Q101C was prepared as described in "MATERIALS AND METHODS." The excitation and emission wavelengths were 330 nm and 450 nm, respectively. Solid circles: 1.5 μM IAANS-Q101C No nucleotide, open circles: 1.5 μM IAANS-Q101C + ATP, crosses: 1.5 μM IAANS-Q101C + ADP.

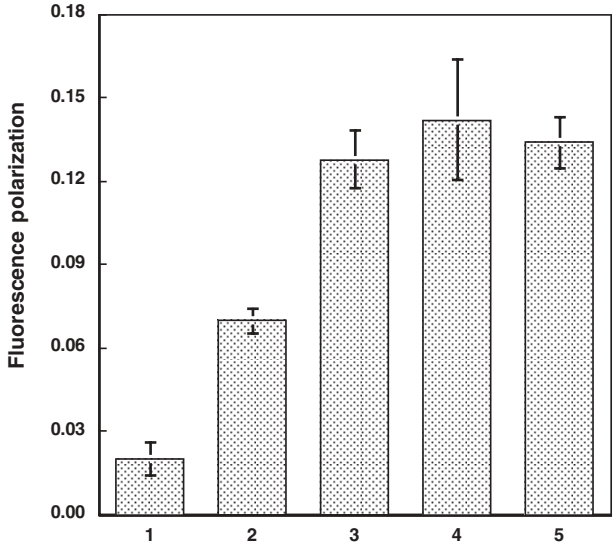

Fig. 8. **Fluorescence emission polarization of IAANS attached to 101C in L5.** (1) 1.5 μM free IAANS; (2) 1.5 μM IAANS-Q101C + 6 M guanidine-HCl; (3) 1.5 μM IAANS-Q101C, no nucleotide; (4) 1.5 μM IAANS-Q101C + 1 mM ATP; (5) 1.5 μM IAANS-Q101C + 1 mM ADP. Samples were measured in a buffer of 120 mM NaCl, 30 mM Tris-HCl, pH 7.5, and 2 mM $MgCl_2$ at 25°C. The excitation and emission wavelengths were 330 nm and 450 nm, respectively. Data are mean ± SD of three to six experiments.

nature of L5 conformational changes related to function remains unclear.

In the present study, we used a fluorescent probe to monitor nucleotide-induced conformational changes in L5. We employed the environmentally-sensitive fluorescent probe IAANS, which specifically attaches to the sulfhydryl group of the cysteine residue. The fluorescence intensity, and to a lesser extent, the emission wavelength of the conjugate, tend to be very sensitive to substrate binding, folding and unfolding of protein (*12*, *22*), and association of the labeled protein with other protein (*11*). IAANS has been widely used for protein structural studies, particularly of contractile proteins (*13*, *23*, *24*). As expected, IAANS successfully detected conformational changes in L5 of kinesin. IAANS attached to 101C of rice kinesin detected L5 conformational change based on changes in its fluorescence intensity and fluorescence maximum. The maximum fluorescence was blue-shifted. From the known general properties of IAANS, it was presumed that the environment around the fluorescent probe becomes to more hydrophobic upon binding of nucleotides. In confirmation of this assumption, the fluorescent polarization, which reflects the mobility of the fluorescent probe, was found to increase slightly in the presence of nucleotides, indicating a reduction of the rotational mobility of probes. On the other hand, the fluorescence intensity was significantly reduced following the addition of nucleotides. Moreover, fluorescence quenching experiments suggested that the fluorescent probe moved to a region which is more accessible for acrylamide upon addition of nucleotides. These results were inconsistent with the experimental data of fluorescence polarization and blue-shifed fluorescence maximum. One possible explanation for the incompatibility might involved the fluorescence from another IAANS bound nonspecifically to kinesin. The fluorescence from the two IAANS molecules bound to different sites may show different characteristics. Indeed, IAANS slightly bound to the intrinsic cysteine residue or other amino acids residues in addition to the destination cysteine 101C. However, this possibility is excluded by the fact that the fluorescence from the nonspecific binding of IAANS is negligibly small, as shown in Fig. 4A. Another possibility, based on our recent unpublished crystallographic analysis of the rice kinesin motor domain, is that nucleotide binding may induce a conformational change of L5 that allows the bound IAANS to make contact with the side chains of neighboring amino acids, thereby quenching the fluorescence intensity and reducing quantum yield. For IAANS, the side chains of basic amino acids are candidates. Indeed, the basic amino acids residues of Arg 102, Arg 61 and Lys 112 are located within 2–8 angstrom from Gln 101 (unpublished data). It is possible that nucleotide binding induces the conformational change of L5, and the sulfonic acid of IAANS bound to 101C in L5 makes a salt bridge with the neighboring basic amino acid side chain. The salt bridge would significantly affect the quantum yield of IAANS and also restrict the movement of the fluorophore. This is quite consistent with the results of fluorescence intensity and fluorescence polarization. Moreover, the aliphatic side chain of lysine or arginine in the salt bridge would make the environment of IAANS hydrophobic, resulting in the blue-shift of fluorescence maximum.

Our results demonstrated that L5 of rice kinesin changes its conformation upon addition of nucleotides. Moreover,

there was a difference in the magnitude of fluorescence intensity change between ADP and ATP, reflecting the formation of a kinesin·ADP state and the equilibrium state of multiple ATPase intermediates. The results suggest that L5 changes its conformation during ATP hydrolysis. We performed the same examination of mouse brain L5 kinesin. IAANS attached to H101C in L5 of mouse kinesin also showed apparent fluorescence decrease upon addition of nucleotides as shown in Fig. 4B. Moreover, the magnitude of the fluorescence change was almost the same or slightly more substantial. Although the L5 of rice kinesin is three amino acids shorter than that of mouse brain kinesin, it is plausible that it changes its conformation in a similar manner during ATP hydrolysis. Moreover, we demonstrated previously that the fluorescence spectrum of Trp 100 in L5 of mouse brain kinesin changed significantly in a nucleotide-dependent manner (unpublished data). On the other hand, the point mutation of Leu 105 to Trp had a significant affect on ATPase activity. Therefore, loop L5 seems to be an important region in the motor domain of kinesin and appears to determine the enzymatic characteristics.

REFERENCES

1. Kull, F.J., Val, R.D., and Fletterick, R.J. (1998) The case for a common ancestor: kinesin and myosin motor proteins and G proteins. *J. Muscle Res. Cell Motil.* **19**, 877–886
2. Kozielski, F., Sack, S., Marx, A., Thormahlen, M., Schonbrunn, E., Biou, V., Thompson, A., Mandelkow, E.M., and Mandelkow, E. (1997) The crystal structure of dimeric kinesin and implications for microtubule-dependent motility. *Cell* **91**, 985–994
3. Sack, S., Muller, J., Marx, A., Thormahlen, M., Mandelkow, E.M., Brady, S.T., and Mandelkow, E. (1997) X-ray structure of motor and neck domains from rat brain kinesin. *Biochemistry* **36**, 16155–16165
4. Kull, F.J., Sablin, E.P., Lau, R., Fletterick, R.J., and Vale, R.D. (1996) Crystal structure of the kinesin motor domain reveals a structural similarity to myosin. *Nature* **380**, 550–555
5. Vale, R.D. (1996) Switches, latches, and amplifiers: common themes of G proteins and molecular motors. *J. Cell Biol.* **135**, 291–302
6. Furch, M., Fujita-Becker, S., Geeves, M.A., Holmes, K.C., and Manstein, D.J. (1999) Role of the salt-bridge between switch-1 and switch-2 of *Dictyostelium* myosin. *J. Mol. Biol.* **290**, 797–809
7. Maruta, S. and Homma, K. (1998) A unique loop contributing to the structure of the ATP-binding cleft of skeletal muscle myosin communicates with the actin-binding site. *J. Biochem.* **124**, 528–533
8. Maruta, S. and Homma, K. (2000) Conformational changes in the unique loops bordering the ATP binding cleft of skeletal muscle myosin mediate energy transduction. *J. Biochem.* **128**, 695–704
9. Song Y.H., Marx A., Muller J., Woehlke G., Schliwa M., Krebs A., Hoenger A., and Mandelkow E. (2001) Structure of a fast kinesin: implications for ATPase mechanism and interactions with microtubules. *EMBO J.* **20**, 6213–25
10. Umeki, N., Nakayama, Y., Kondo, K., Mitsui, T., and Maruta, S. (2005) Purification and characterization of the plant specific kinesin. *Biophys. J.* **88**, 651a
11. Zot, H.G., Aden, R., Samy, S., and Puett, D. (1990) Fluorescent adducts of wheat calmodulin implicate the amino-terminal region in the activation of skeletal muscle myosin light chain kinase. *J. Biol. Chem.* **265**, 14796–14801
12. Bock, P.E., Day, D.E., Verhamme, I.M.A., Bernardo, M.M., Olson, S.T., and Shore, J.D. (1996) Analogs of human plasminogen that are labeled with fluorescence probes at the catalytic site of the zymogen. *J. Biol. Chem.* **271**, 1072–1080
13. Hazard, A.H., Kohout, S.C., Stricker, N.L., Putkey, J.A., and Falke, J.J. (1998) The kinetic cycle of cardiac troponin C: Calcium binding and dissociation at site II trigger slow conformational rearrangements. *Protein Sci.* **7**, 2451–2459
14. Shibuya, H., Kondo, K., Kimura, N., and Maruta, S. (2002) Formation and characterization of kinesin·ADP·fluorometal complexes. *J. Biochem.* **132**, 573–579
15. Hackney D.D. (1988) Kinesin ATPase: Rate-limiting ADP release. *Proc. Natl. Acad. Sci. USA* **85**, 6314–6318
16. Lehrer, S.S. and Leavis, P.C. (1978) Solution quenching of protein fluorescence. *Methods Enzymol.* **49**, 222–236
17. Stern, O. and Volmer, M. (1919) Uber die abklingungszeit der fluoreszenz. *Phys. Z.* **20**, 183
18. Putkey, J.A., Potter, J.D., and Kerrick, W.G.L. (1997) Fluorescent probes attached to cys 35 or cys 84 in cardiac troponin C are differentially sensitive to Ca^{2+}-dependent events in vitro and in situ. *Biochemistry* **36**, 970–978
19. Youngburg, G.E. and Youngburg, M.V. (1930) Phosphorous metabolism: I. A system of blood phosphorus analysis. *J. Lab. Clin. Med.* **16**, 158–166
20. Majima, E., Shinohara, Y., Yamaguchi, N., Hong, Y.M., and Terada, H. (1994) Importance of loops of mitochondrial ADP/ATP carrier for its transport activity deduced from reactivities of its cysteine residues with the sulfhydryl reagent eosin-5-maleimide. *Biochemistry* **33**, 9530–9536
21. Simon, S. (1994) Enter the swinging gate. *Nature* **371**, 103–104
22. Bhattacharyya, A.M. and Horowits, P. (2000) Alteration around the active site of rhodanese during ultra-induced denaturation and its implications for folding. *J. Biol. Chem.* **275**, 14860–14864
23. Johnson, J.D., Collins, J.H, Robertson, S.P., and Potter, J.D. (1980) A fluorescent probe study of Ca^{2+} binding to the Ca^{2+}-specific sites of cardiac troponin and troponin C. *J. Biol. Chem.* **255**, 9635–9640
24. Abbott, M.B., Gaponenko, V., Abusamhadneh, E., Finley, N., Li, G., Dvoretsky, A., Rance, M., Solaro, R.J., and Rosevear, P.R. (2000) Regulatory domain conformational exchange and linker region flexibility in cardiac troponin C bound to cardiac troponin I. *J. Biol. Chem.* **275**, 20610–20617